

Wave Attenuation by Suspended Flexible Vegetation

Zhilong Wei*, Yanlin Shao

Technical University of Denmark, Kgs. Lyngby, 2800, Denmark

*zhilwei@dtu.dk

1 INTRODUCTION

At the 39th IWWF (Scotland, 2024), we presented an analytical model for wave attenuation by cultivated seaweeds in which blades were idealized as rigid bars hinged at their upper ends [1]. This assumption is appropriate when buoyancy dominates bending stiffness. In the present work, the blades are modeled as Euler–Bernoulli beams, preserving buoyancy while allowing flexible deformation. Quadratic drag is linearized on an energy-conservation basis in regular waves and an extension is made to irregular waves via stochastic linearization. The cross-sectional drag coefficient C_D is selected primarily based on the local Keulegan–Carpenter (KC) number. Compared with the rigid-bar idealization, the Euler–Bernoulli beam model yields more physically realistic blade deflections. Specifically, motion amplitudes in the lower part are smaller than those in the upper part, since the wave kinematics decay exponentially toward the seabed.

2 THEORY

The general problem is illustrated in Fig. 1. A suspended canopy of cultivated seaweed partitions the water column into three layers. The governing equations and boundary conditions are annotated in each layer.

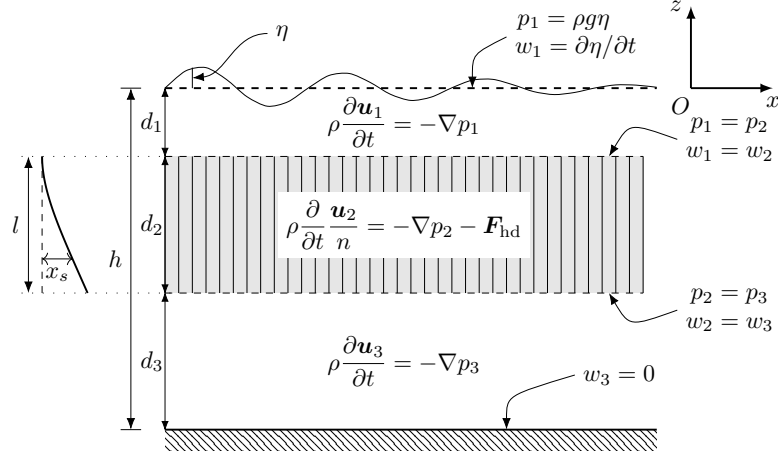


Figure 1: Schematic of the physical problem.

2.1 Governing Equations

As in [1, 2], the fluid motion is governed by the linearized NS equations with neglected advection terms and viscous stresses. A first-order (linear) analytical solution is thus possible. Assuming small blade deflection, the interfaces between the canopy region and the water layers are also linearized. See [1, 2] for further details.

In contrast to [1, 2], each blade here is modeled as a prismatic Euler–Bernoulli cantilever. Let $s = -(z + d_1) \in [0, l]$ be the arclength measured downward from the clamped top ($s = 0$) to the free tip ($s = l = d_2$). In addition to flexural stiffness, the effective gravity in water plays an important role owing to the high flexibility of seaweed. The governing equation of motion of the seaweed blade reads

$$\mu \frac{\partial^2 x_s}{\partial t^2} - \frac{\partial}{\partial s} \left(T \frac{\partial x_s}{\partial s} \right) + EI \frac{\partial^4 x_s}{\partial s^4} = \frac{F_{hd,x}}{N}, \quad (1)$$

where E is Young's modulus, I the second moment of area, ρ_s the seaweed material density, $\mu = \rho_s A_s$ the blade mass per unit length, and $F_{\text{hd},x}$ is the hydrodynamic force on the blade, estimated by Morison's equation in this study. The axial tension T due to weight and buoyancy in water is $T = B(l - s)$, where $B = (\rho_s - \rho)gA_s$ is the effective weight per unit length in water. Since $\rho_s > \rho$ for seaweeds [3], $T(s)$ remains positive, so that the submerged weight provides a tensile restoring force. The linear tension T introduces a variable-coefficient term in the ODE, preventing a simple explicit solution. Here, we neglect tension variation along the blade and use the mid-span tension at $s = l/2$ to represent the restoring force due to tension and curvature, i.e., we set $T = 1/2Bl$. The governing equation of motion of the blade now reads:

$$\left(\mu + \rho C_M \frac{\pi}{4} b^2\right) \frac{\partial^2 x_s}{\partial t^2} - \frac{1}{2} Bl \frac{\partial^2 x_s}{\partial s^2} + EI \frac{\partial^4 x_s}{\partial s^4} = \rho \left(C_M \frac{\pi}{4} b^2 + A_s\right) \frac{\partial}{\partial t} \frac{u_2}{n} + \frac{1}{2} \rho C_D b \left| \frac{u_2}{n} - \frac{\partial x_s}{\partial t} \right| \left(\frac{u_2}{n} - \frac{\partial x_s}{\partial t} \right). \quad (2)$$

The cantilever boundary conditions are $x_s = \partial x_s / \partial s = 0$ at $s = 0$ and $\partial^2 x_s / \partial s^2 = \partial^3 x_s / \partial s^3 = 0$ at $s = l$. Note that we retain the physical free-tip boundary conditions even though the interior tension is assumed constant. While approximating the linearly varying tension with a constant value is a simplification, its accuracy can be assessed against exact solutions obtained via power-series methods (Bessel-type formulations).

2.2 Solutions

All governing equations are linear except for the quadratic drag terms in Eq. (2). We introduce an equivalent linear drag coefficient and let

$$D = \frac{\int_{-(d_1+d_2)}^{-d_1} \frac{1}{2} C_D b N n^{-2} |u_2 - n \partial x_s / \partial t|^3 dz}{\int_{-(d_1+d_2)}^{-d_1} (u_2 - n \partial x_s / \partial t)^2 dz}, \quad A_1 = C_M \frac{\pi}{4} b^2 N, \quad A_2 = A_s N, \quad (3)$$

Here D is defined such that the work done by the linearized load on the vegetation over one wave period is identical to that done by the quadratic drag. Eq. (3) has been widely used for analytical solutions to wave attenuation by vegetation. For sharp-edged sections in oscillatory flows, C_D depends primarily on KC, and is comparatively less sensitive to the Reynolds number. Accordingly, we adopt the following KC-dependent empirical formula [4] to estimate the instantaneous sectional $C_D = \max(8\text{KC}^{-1/3}, 1.95)$, where $\text{KC} = U_r T / b$ is based on the local blade width b , where U_r is the amplitude of the normal component of the structure-fluid relative velocity. $C_D = 8\text{KC}^{-1/3}$ is based on the experimental results of flat plates with small KC values following [4], while $C_D = 1.95$ represents the asymptotic value as $\text{KC} \rightarrow \infty$. In general, D from Eq. (3) is obtained iteratively.

We consider steady-state solutions, so all fields are harmonic functions oscillating with the same wave frequency. The free-surface elevation η is expressed in the form (periodic in time, progressive and attenuating in space) $\eta = \Re \{ H_0 / 2 e^{i(\omega t - kx)} \}$, where $k = k_r + ik_i$ is the complex wave number, ω is the (real) angular wave frequency, and H_0 is the incident wave height. The corresponding local wave height $H(x)$ decays exponentially and is expressed as $H(x) = H_0 e^{k_i x}$, with $k_i < 0$ for attenuation.

As in linear wave theory, u_j , w_j , and p_j are proportional to $e^{i(\omega t - kx)}$ and take the separable forms $\{u_j, w_j, p_j\}(x, z, t) = \Re \{ \{U_j(z), W_j(z), P_j(z)\} e^{i(\omega t - kx)} \}$, and the blade deflection is represented as $x_s = \Re \{ X_s(z) e^{i(\omega t - kx)} \}$. Consequently, the relative velocity amplitude for C_D is given by $U_r = |U_2 - i\omega n X_s|$.

The velocities must satisfy the continuity equation, which leads to

$$\frac{d^2 P_j}{dz^2} - k^2 P_j = 0, \quad j = 1, 3; \quad \frac{d^2 P_2}{dz^2} - \kappa^2 P_2 + \varsigma X_s = 0, \quad (4)$$

where

$$\left(\frac{\kappa}{k}\right)^2 = \frac{n}{(A_1 + A_2 + 1) - iD/\omega}, \quad \varsigma = \rho k \omega^2 \frac{n(A_1 - iD/\omega)}{i(A_1 + A_2 + 1) + D/\omega}. \quad (5)$$

Similarly, the boundary conditions are $P_1 = g/\omega^2 dP_1/dz$ at $z = 0$, $P_1 = P_2$ and $dP_1/dz = dP_2/dz$ at $z = -d_1$, $P_2 = P_3$ and $dP_2/dz = dP_3/dz$ at $z = -(d_1 + d_2)$, and $dP_3/dz = 0$ at $z = -h$. Meanwhile, the ODE for X_s (in $z = -(d_1 + s)$) is deduced from Eq. (2) after drag linearization as

$$-\omega^2 \left(\mu + \rho \frac{A_1}{N} \right) X_s - \frac{1}{2} Bl \frac{d^2 X_s}{dz^2} + EI \frac{d^4 X_s}{dz^4} = i\omega \frac{\rho}{N} (A_1 + A_2) \frac{U_2}{n} + \frac{\rho D}{N} (U_2 - i\omega n X_s). \quad (6)$$

Substituting U_2 expressed in terms of P_2 into the equation above and rearranging, we obtain

$$\frac{d^4 X_s}{dz^4} - \frac{1}{2} \frac{Bl}{EI} \frac{d^2 X_s}{dz^2} + \lambda^4 X_s + \xi P_2 = 0, \quad (7)$$

where

$$\lambda^4 = -\frac{\omega^2}{EI} \left(\mu + \frac{\rho}{N} \frac{iA_1 + D/\omega(1 - A_2 - A_2^2)}{i(A_1 + A_2 + 1) + D/\omega} \right), \quad \xi = \frac{1}{EI} \frac{kn}{N} \frac{(A_1 + A_2)/n - iD/\omega}{i(A_1 + A_2 + 1) + D/\omega}. \quad (8)$$

The boundary conditions are $X_s = \partial X_s / \partial z = 0$ at $z = -d_1$ and $\partial^2 X_s / \partial z^2 = \partial^3 X_s / \partial z^3 = 0$ at $z = -(d_1 + d_2)$. In conclusion, we have a system of four ODEs:

$$\frac{d^4}{dz^4} \begin{bmatrix} 0 \\ 0 \\ 0 \\ X_s \end{bmatrix} + \frac{d^2}{dz^2} \begin{bmatrix} 1 & 0 & 0 & 0 \\ 0 & 1 & 0 & 0 \\ 0 & 0 & 1 & 0 \\ 0 & 0 & 0 & -\frac{1}{2} \frac{Bl}{EI} \end{bmatrix} \begin{bmatrix} P_1 \\ P_2 \\ P_3 \\ X_s \end{bmatrix} + \begin{bmatrix} -k^2 & 0 & 0 & 0 \\ 0 & -\kappa^2 & 0 & \zeta \\ 0 & 0 & -k^2 & 0 \\ 0 & \xi & 0 & \lambda^4 \end{bmatrix} \begin{bmatrix} P_1 \\ P_2 \\ P_3 \\ X_s \end{bmatrix} = \begin{bmatrix} 0 \\ 0 \\ 0 \\ 0 \end{bmatrix}. \quad (9)$$

The unknowns P_2 and X_s are coupled with each other but not with P_1 and P_3 by the governing equations, although P_j are coupled through the boundary conditions. In total, there are ten unknown coefficients (two for P_1 , two for P_3 , six for coupled P_2 and X_s) and one dispersion relation, which are determined from the eleven boundary conditions. The regular-wave solution can be extended to irregular seas by applying stochastic linearization to the quadratic drag term; see more details in [1, 2].

3 RESULTS

The analytical model is validated against the experiments of [3], which examined regular wave propagation over a suspended kelp farm. The physical setup comprised 20 longlines ($L_v = 3.8$ m) with silicone model blades ($\rho_s = 1.20$ kg/m³, $E = 2.04$ MPa). In the present model, the blades are represented as equivalent single beams with dimensions 9.66 cm \times 0.95 mm \times 0.1 mm and a distribution density of $N = 5263$ m⁻². A constant added-mass coefficient $C_M = 0.5$ is adopted. Fig. 2 compares the analytical predictions of the wave height transmission ratio (HTR, ratio of wave height at the downstream edge of the canopy to the incident wave height H_0) and the wave decay coefficient K_D (obtained from $\text{HTR} = 1/(1 + K_D H_0 L_v)$) against 14 experimental cases, using both the Euler–Bernoulli beam model and the rigid bar model. The results from a two-way coupled numerical model [5] (time-domain solver, fully non-linear structure model, quadratic drag) using the same C_M value are also provided. The strong correlation ($R^2 = 0.94$ for HTR) confirms the validity of using $C_M = 0.5$. By contrast, the rigid-bar model requires $C_M > 1.0$ to obtain comparable agreement (e.g., $R^2 = 0.54$ for HTR [2]). Although tuning C_M improves the fit (e.g., $C_M = 2.0$ yields $R^2 = 0.71$ for HTR), it still does not match the performance achieved by the Euler–Bernoulli formulation. Overall, the Euler–Bernoulli formulation predicts wave attenuation more accurately than the rigid-bar idealization. The corresponding blade deflections at $x = 0$ are shown in Fig. 3 for the 14 cases, further indicating that the Euler–Bernoulli beam model yields more physically realistic deformation. Additional results will be presented at the workshop.

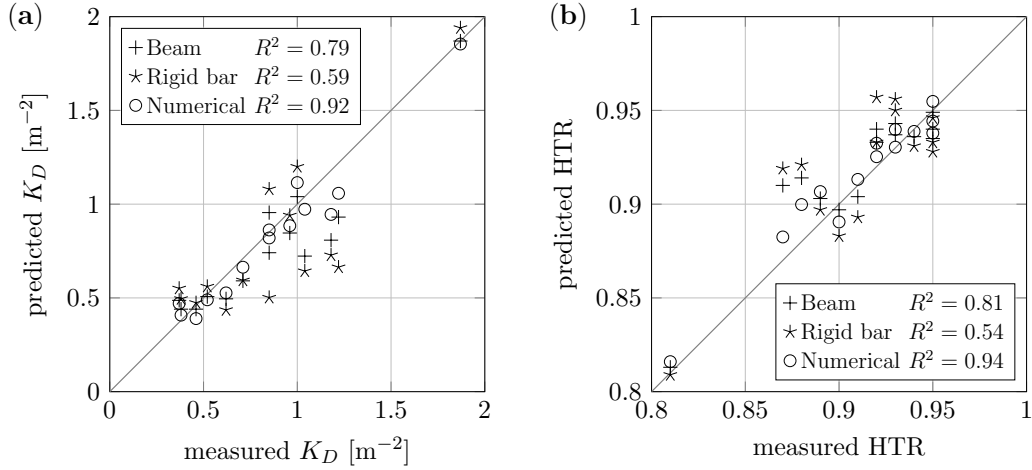


Figure 2: Comparison of analytical (both Euler–Bernoulli beam model and rigid bar model), numerical, and experimental results for (a) wave decay coefficient K_D and (b) wave transmission ratio (HTR).

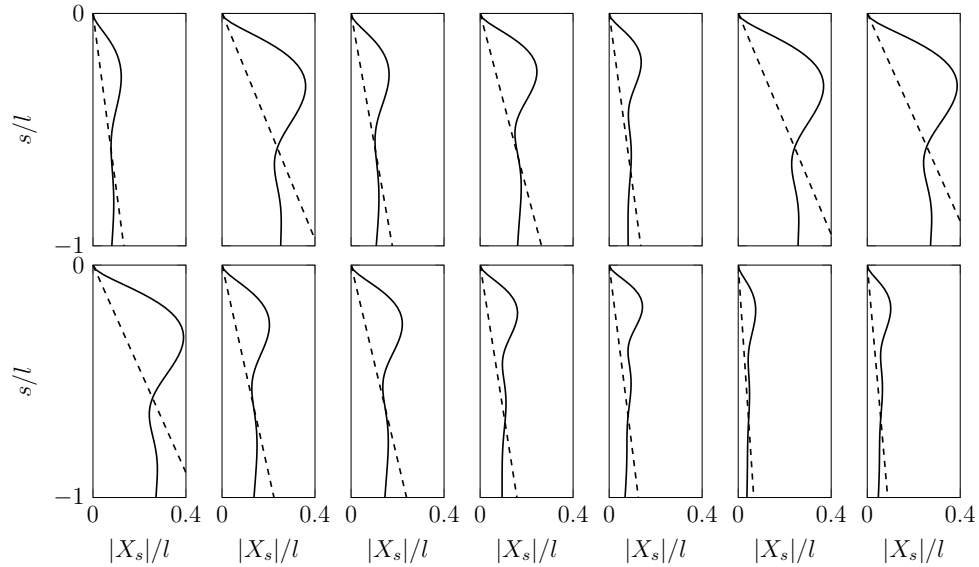


Figure 3: Comparison of the blade deflection at $x = 0$ for the 14 cases of [3] calculated using the Euler–Bernoulli beam model (solid) and the rigid bar model (dashed).

REFERENCES

- [1] Shao, Y., Weiss, M., and Wei, Z. Wave Attenuation by Cultivated Seaweeds: A Linearized Analytical Solution. In *Proceedings of 39th International Workshop on Water Waves and Floating Bodies* (St. Andrews, United Kingdom, Apr. 2024), IWWFBB.
- [2] Wei, Z., Weiss, M., Kristiansen, T., Kristiansen, D., and Shao, Y. Jan. 2025. *Wave attenuation by cultivated seaweeds: A linearized analytical model. Coastal Engineering* 195, 104642.
- [3] Zhu, L., Lei, J., Huguenard, K., and Fredriksson, D. W. 2021. *Wave attenuation by suspended canopies with cultivated kelp (Saccharina latissima). Coastal Engineering* 168, 103947.
- [4] Graham, J. M. R. Mar. 1980. *The forces on sharp-edged cylinders in oscillatory flow at low Keulegan–Carpenter numbers. Journal of Fluid Mechanics* 97(02), 331.
- [5] Wei, Z., Shao, Y., Kristiansen, T., and Kristiansen, D. Oct. 2024. *An efficient numerical solver for highly compliant slender structures in waves: Application to marine vegetation. Journal of Fluids and Structures* 129, 104170.